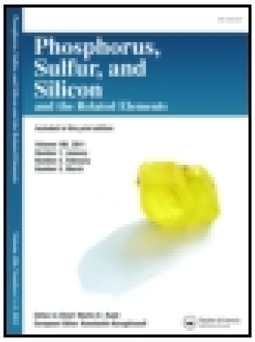

Taylor & Francis
Taylor & Francis Group

Phosphorus, Sulfur, and Silicon and the Related Elements

ISSN: 1042-6507 (Print) 1563-5325 (Online) Journal homepage: http://www.tandfonline.com/loi/gpss20

Introduction Of PEG-SANM Nanocomposite As A New And Highly Efficient Reagent For The Promotion Of The Silylation Of Alcohols And Phenols And Deprotection Of The Silyl Ethers

Farhad Shirini, Abdollah Fallah Shojaei & Seyedeh Zahra Dalil Heirati

To cite this article: Farhad Shirini, Abdollah Fallah Shojaei & Seyedeh Zahra Dalil Heirati (2016): Introduction Of PEG-SANM Nanocomposite As A New And Highly Efficient Reagent For The Promotion Of The Silylation Of Alcohols And Phenols And Deprotection Of The Silyl Ethers, Phosphorus, Sulfur, and Silicon and the Related Elements, DOI: 10.1080/10426507.2015.1119141

To link to this article: http://dx.doi.org/10.1080/10426507.2015.1119141

INTRODUCTION OF PEG-SANM NANOCOMPOSITE AS A NEW AND HIGHLY EFFICIENT REAGENT FOR THE PROMOTION OF THE SILYLATION OF ALCOHOLS AND PHENOLS AND DEPROTECTION OF THE SILYL ETHERS

Farhad Shirini[1,*] Abdollah Fallah Shojaei[1,*] Seyedeh Zahra Dalil Heirati[1]

[1]Department of Chemistry, College of Science, University of Guilan, Rasht 41335, Iran.

[*]E-Mail: shirini@guilan.ac.ir (F. Shirini); a-fallah@guilan.ac.ir (A. Fallah Shojaei); Fax: +98 131 3220066

Abstract

Poly (ethylene glycol)-sulfonated sodium montmorillonite (PEG-SANM) nanocomposite was prepared by a simple method and characterized using XRD, TGA, SEM, TEM and FT-IR techniques. After preparation and characterization, this reagent was used as a highly efficient and reusable solid acid catalyst for the chemoselective silylation of alcohols and phenols and deprotection of the obtained silyl ethers. The method offers several advantages including high to excellent yields of the products, short reaction times, easy preparation of the catalyst and easy work-up procedure. Additionally, the catalyst can be recycled and reused at least for five times without significant decrease in the catalytic activity.

Keywords

Nanocomposite, PEG, SANM, silylation, deprotection.

Clay/polymer nanocomposites are a typical example of nanocomposites. This class of materials uses smectite-type clays, such as montmorillonite, as a filler to enhance the properties of polymers. Polymer/montmorillonite nanocomposites have attracted great interests in recent years, both as novel materials with improved properties and as ideal systems for the study of polymer behavior in a nanoscopically confined space. [1-3]

Different scientific communities, ranging from medical to materials science and engineering, are interested in polymer modified clays and they have deeply investigated these hybrid organic--inorganic systems. [4-10] Depending on the preparation method and the nature of the components used containing a polymer matrix and layered silicate, two types of nanocomposites can be gained. When a single, or occasionally more extended, polymer chain is intercalated between the silicate layers, intercalated structures are formed, that is a well-ordered multilayer structure of alternating polymeric and silicate layers, with a repeat distance among them. Instead, when the silicate layers are well separated from one another and separately dispersed in the continuous polymer matrix, exfoliated or delaminated structures are gained. [11-14]

Poly (ethylene glycol) (PEG) is a polymer with good physicochemical and biological properties including the solubility in water and organic solvents, hydrophilic properties, and lack of toxicity, which allow PEG to be used as a catalyst and /or solvent in many organic reactions. [15-17] In particular, the intercalation of poly (ethylene glycol) into montmorillonite (MMT) has been studied extensively in many researches. This is due to its potential applications as electrolytes in solid-state batteries. [18-22] PEG/MMT nanocomposites show significant increase in the interlayer space of montmorillonite due to incorporation of poly (ethylene glycol) chains within it. In this case, the conformation of PEG chains confined into the interlayer space of montmorillonite is not helical as in crystalline PEG. [23] Recently, the development and characterization of polymer-clay nanocomposites received special attention, but among different researches on these materials, there are a few reports in terms of their application as heterogeneous catalysts. [24] When synthesizing polymer--clay nanocomposites, structural characterization of the products, regardless of their properties, is important.

The protection of the hydroxyl group in alcohols and phenols is an important technique during multistep synthesis. Among the different methodologies for the protection of hydroxyl groups, the transformation of alcohols to the corresponding silyl ethers is a popular procedure. [25] 1,1,1,3,3,3-Hexamethyldisilazane (HMDS) is a stable, inexpensive, and commercially available reagent that can be used for the conversion of the hydroxyl groups to their corresponding silyl ethers (TMS ethers), but it suffers from the low reactivity in the silylation reaction. Therefore, a variety of catalysts such as Au/TiO_2 [26], aspartic acid [27], γ-Fe_2O_3@SiO_2-$(CH_2)_3$NH-Sn(*n*-Bu)$_3$ [28], Boric acid [29], SiO_2-Cl [30], H-β zeolite [31], and $Bi(OTf)_3$ [32] have been developed for the activation of this reagent. Although the silylation ability of HMDS has been improved using these methods, some problems such as long reaction times, the use of a non-recoverable catalyst, drastic reaction conditions, need for organic solvents, inability to catalyze the reverse reaction, and the use of excess amounts of the silylating agents still need to be overcome. Recently, some of the new effective heterogeneous solid acid catalysts have been designed for the silylation reaction that can overcome the above problems. For instance, Zareyee and Karimi reported the application of recoverable sulfonic acid functionalized ordered mesoporous silica (MCM-41-Pr-SO_3H) [33] and propyl sulfonic acid functionalized nanostructured SBA-15 (SBA-15-Ph-Pr-SO_3H) [34] for the efficient silylation of alcohols and phenols.

In our previous research, sulfonic acid-functionalized ordered nanoporous Na^+-montmorillonite (SANM) was demonstrated as an efficient reusable catalyst for the silylation of alcohols and phenols. [35] In continuation of our work on SANM and other heterogeneous solid acid catalysts [36-39], with the aim of obtaining a new catalyst, we prepared and characterized PEG-SANM nanocomposite, and then examined its ability as a new heterogeneous solid acid catalyst in the chemoselective silylation of alcohols and phenols and deprotection of the obtained products.

Fig. 1 presents the FT-IR spectra of PEG, SANM and the PEG-SANM nanocomposite. In the case of crystalline PEG, the wagging vibrations of the CH_2 occur at 1352 and 1284 cm^{-1}. The CH_2 rocking vibrations appear at 953 cm^{-1}. The band between 1050 and 1150 cm^{-1} that centered at 1109 cm^{-1} is due to C-O-C stretching vibrations. The bands appeared at 1352 and 953 cm^{-1} arise from the helical PEG chain. The occurrence of these bands confirms the helical conformations of PEG chains in crystalline state. [11-14]

In the infrared spectra of the PEG-SANM nanocomposite, some bands shift or merge because the PEG is confined in the interlayer spaces of SANM. For example, the wagging vibrations of the CH_2 appear as only single band at 1357 cm^{-1}. The bands related to helical conformation (1352 and 953 cm^{-1}) disappear because the PEG chains confined into the interlayer space of SANM lost their helical conformation and became disorder. The absence of these bands confirms that the PEG chains have been successfully intercalated into the interlayer space of SANM.

In the case of SANM, the broad band around 1050 cm^{-1} is due to the overlapping of Si-O and S-O bands that is not affected in the infrared spectra of the PEG-SANM nanocomposite.

The XRD patterns of the PEG-SANM nanocomposite, SANM, Na^+-MMT, and PEG-6000 are shown in Fig. 2. The interlayer distance (d) of the PEG-SANM nanocomposite, Na^+-MMT, and SANM calculated from Bragg's formula: $n\lambda = 2d \sin \theta$. The basal spacing for the Na^+-MMT is 0.98 nm with $2\theta = 9°$. Because of the intercalation of the sulfonic acid moiety into montmorillonite interlayer spaces, the basal spacing of SANM became obviously bigger than that of Na^+-MMT (1.29 nm, $2\theta = 7°$). [35] The PEG-SANM nanocomposite shows a sharp peak at $2\theta = 5°$ with d = 1.77 nm, indicating an increase in the basal spacing compared to SANM. This increase can be due to the intercalation of the PEG chains into the interlayer spacing of SANM, which leads to a shift of the diffraction peak towards lower angle, according to Bragg's law. PEG shows two crystalline reflections at $2\theta = 19.2°$ and $2\theta = 23.4°$. Absence of any PEG crystal peaks in the XRD pattern of the PEG-SANM nanocomposite indicates that a large amount of PEG are intercalated into the SANM and free PEG on the SANM surface is negligible. The 0.48 nm expansion is consistent with an adsorbed monolayer PEG between the clay surfaces.

Fig. 3 provides the TGA and DTG curves of PEG-SANM nanocomposite. The complete thermal decomposition of pure PEG-6000 is a one-step process that is started from 175°C, and is completed at 300°C. [8] For SANM there is a weight loss in the range of 25-240°C, attributed to the loss of the bonded H_2O within the interlayer spaces and a weight loss that started from 240°C, which can be attributed to the decomposition of --SO_3H groups anchored to the clay surface. [35] However, the trend of weight loss curve of the PEG-SANM nanocomposite is different from those of the pure PEG-6000 and SANM. The PEG-SANM nanocomposite has four weight loss steps. The first weight loss is observed in the range of 75-140°C (0.7% weight loss), attributed to the loss of the physically adsorbed water. The second weight loss, between 140 and 195°C (1.8% weight loss) which is possibly corresponding to the loss of the bonded H_2O within the interlayer spaces. The third weight loss in the range of 195-380°C (19.5% weight loss) can be a result of the thermal decomposition of the --SO_3H groups and the fourth weight loss, which started from 380°C can be attributed to the thermal decomposition of PEG-6000. According to the obtained results it was found that decomposition of the PEG-6000 in the PEG-SANM nanocomposite requires higher temperature compared to the pure polymer. This shows that the thermal stability of the PEG confined into the interlayer spacing of SANM has been increased.

It is well known that SEM method is important for investigation of surface morphology-structure-property relationships of polymer/clay nanocomposites. The scanning electron microscopy (EM) photographs of the PEG-SANM nanocomposite are presented in the Supplemental Materials in Figure S2 (available online in Supplemental Materials). Darker and lighter areas indicate SANM and PEG, respectively. As seen in the images, the amount of polymer into the SANM layers is more than that on the SANM surface which is consistent with the results of X-ray.

TEM is required to image the clay platelets and fully identify the type of nanocomposites that has been produced. To further confirm the dispersion of polymer fragments in the SANM, TEM investigations are also required. Since the silicate layers are composed of heavier elements (Al, Si and O) than the interlayer and surrounding matrix (C, H and O), they appear darker in the images. Therefore, when nanocomposites are formed, the intersections of the silicate sheets are seen as dark lines which are the cross sections of the silicate layers. [7] The TEM images presented in the Supplemental Materials in Figure S 3 (available online in Supplemental Materials) show the formation of an exfoliated and intercalated nano-morphology between interlayer spaces of SANM. Black points (agglomerated clay layers) in TEM images are associated with intercalated structures. The presence of single and partially agglomerated clay layers indicates the formation of individual dispersion of delaminated clay platelets. According to TEM images, it was found that predominated structure of nanocomposite is intercalated nano-morphology.

The acid sites content of the PEG-SANM nanocomposite and SANM were estimated by back titration using HCl (0.337 N). [24] In this method, 10 mL of NaOH (0.130 N) was added to 0.05 g of the PEG-SANM nanocomposite and SANM and stirred for 30 min. The catalysts were separated and washed with deionized water. The excess amount of NaOH was titrated with HCl (0.337 N) in the presence of phenol phthalein as indicator. The acid sites content were 2.41 and 4.43 mmol g^{-1} for SANM and the PEG-SANM nanocomposite, respectively. In sulfonated soduim montmorillonite (SANM), $-SO_3H$ groups are randomly scattered into the interlayer spaces of the SANM, and these groups are less accessible for determining the acidic content. When PEG is intercalated between the modified clay interlayer, the $-SO_3H$ groups because of the spatial exclusion are oriented towards the outside of the modified clay. Therefore, more $-SO_3H$ groups are available for determining the acidic content that increases the number of acid sites from 2.41 to 4.43 mmol g^{-1}. In fact, the acidity determination only characterizes the accessible acid sites.

 ACCEPTED MANUSCRIPT

The silylation of alcohols was chosen as a model reaction to test the catalytic activity of the PEG-SANM nanocomposite. In order to optimize the reaction conditions, effects of HMDS and the PEG-SANM nanocomposite amounts on outcome of the silylation of 4-chlorobenzyl alcohol was studied. As shown in Table 1, the amounts of HMDS (0.5 mmol) and the PEG-SANM nanocomposite (8 mg) are appropriate for this reaction.

After optimization of the amounts of HMDS and the catalyst, the effects of the solvent and temperature were also studied in the model reaction. The obtained results clarified that the best results can be obtained under the conditions showed in Scheme 1.

Using the best conditions established above, different types of alcohols were subjected to silylation (Table 2, entries 1-24). Benzylic alcohols (including electron releasing or withdrawing groups and acid sensitive groups) were silylated with relatively high yields (Table 2, entries 1-15). Silylation of primary, secondary and tertiary aliphatic alcohols also proceeded efficiently with good to high yields (Table 2, entries 16-22). This method was also found to be useful for silylation of allylic alcohols, so the carbon-carbon bond remained intact during the course of the reaction (Table 2, entry 23). Also, the catalytic system is applicable for silylation of diols (Table 2, entry 24). Phenols were also successfully converted to their corresponding silyl ethers in high yields under the same reaction conditions (Table 2, entries 25, 26). No elimination and rearrangement by-products were observed at all. Notably, amines and thiols remained unaffected under the reaction conditions (Table 2, entries 27-30). Thus, this method is highly selective for silylation of benzylic, primary, secondary and tertiary aliphatic alcohols and phenols in the presence of amines and thiols. The importance of the selectivity issue in synthetic organic chemistry led us to carry out competitive reactions in order to evaluate the chemoselectivity of

 ACCEPTED MANUSCRIPT

this method (Table 2, entries 31-34). The PEG-SANM nanocomposite also shows capability for the conversion of silyl ethers to the parent alcohols and phenols in MeOH at room temperature with good to excellent yields (Table 2).

In order to show the efficiency of the present method, we compared our obtained results from the silylation of benzyl alcohol with some of those that reported in the literature. As can be seen in Table 3, this method overcomes the disadvantages of other procedures such as long reaction times, low yields, high loading of the catalyst, and excess amounts of HMDS. It is also important to note that although SANM, $HClO_4$--SiO_2, and RiH are able to catalyze the silylation of alcohols and phenols in short reaction times and high yields, but the required amounts of the catalyst are higher than the one used in our catalytic system. As can be seen in Table 3, the promotion of these reactions need 20 mg of SANM, 50 mg of $HClO_4$--SiO_2 and 80 mg of RiH (Table 3, entries 5, 6, and 7), while the required amount of PEG-SANM nanocomposite is only 8 mg. In spite of the utilization of lower amount of boric acid as the catalyst the reaction time is too long (Table 3, entry 2). In the case of SiO_2-Cl and SBA-15-Ph-Pr-SO_3H, the amounts of the catalysts are higher and also the related reaction times are longer (Table 3, entries 3, 4). In all cases, the used amounts of HMDS are higher than that the one used in our procedure.

In conclusion, the PEG-SANM nanocomposite was prepared by a simple method and successfully utilized for the chemoselective silylation of a variety of alcohols and phenols and deprotection of silyl ethers. This procedure led to high product yields in very short reaction times by using lower amounts of the catalyst and HMDS reagent. However, the PEG-SANM nanocomposite has the other important advantages such as easy preparation, reasonable results, outstanding stability, simple workup and reusability.

ACCEPTED MANUSCRIPT

EXPERIMENTAL

General: All chemicals were obtained from Fluka, Merck and Aldrich chemical companies. All yields refer to the isolated pure products. The purity determination of the substrates and reaction monitoring were performed on TLC using silica gel SIL G/UV 254 plates. Products were characterized by comparison of their physical data with authentic samples. Representative IR spectra for the products **2a-2z** are provided in the Supplemental Materials (Figures S 4 -- S 25)

Instrumentation: The FT-IR spectra were run on a VERTEX 70 Bruker company (Germany). Thermogravimetric analyses (TGA) was performed under Argon using STA-503 at a heating rate of 10°C/min. The powder XRD patterns of samples was recorded by a Philips PW 1840 diffractometer using Cu Kα radiation (α = 1.54 Å). The patterns were collected in the range of 0--30° 2θ and continuous scan mode. Transmission electron microscope (TEM) image was obtained on a Philips CM10 transmission electron microscope with an accelerating voltage of 100 kV. Scanning image was obtained on a KYKY-EM3200 microscope.

Preparation and characterization of sulfonated sodium montmorillonite (SANM) [35]:

A 50 mL suction flask charged with sodium montmorillonite (1.0 g, Southern Clay Products) and $CHCl_3$ (5mL) was equipped with a constant pressure dropping funnel containing chlorosulfonic acid (0.30 g, 2.5 mmol) and a gas inlet tube for conducting HCl gas over water. When the reaction mixture was stirred slowly in an ice bath (0°C), chlorosulfonic acid was added drop-wise to this mixture within 30 min. After addition was completed, the mixture was stirred for other 30 min to remove all HCl. Then, the mixture was filtered and washed with methanol (20 mL) and dried at room temperature to afford sulfonated sodium montmorillonite (1.04 g).

Catalyst preparation:

PEG-6000 (1.0 g) was dispersed in ethanol (25 mL) and stirred at 60 °C for 30 min. Then sulfonated sodium montmorillonite (1.0 g) (SANM) was slowly added and the reaction mixture was stirred for 3 h at 60 °C in an oil bath. After the completion of reaction, the reaction mixture was filtered and air-dried at room temperature for 24 h to obtain the PEG-SANM nanocomposite as a white powder (1.8 g).

General procedure for silylation of the alcohols and phenols:

HMDS (0.5 mmol) was added to a stirring mixture of the substrate (1 mmol), and the PEG-SANM nanocomposite (8 mg) in CH_3CN (2 mL) at room temperature. The progress of the reaction was monitored by TLC. After completion of the reaction, the mixture was filtered and the recovered catalyst was washed with acetonitrile and acetone, dried at 80°C and reused for the same reaction. Evaporation of the solvent gave almost pure product. Further purification proceeded by recrystallization to yield pure silyl ether.

General procedure for deprotection of silyl ethers:

A mixture of the substrate (1mmol) and the PEG-SANM nanocomposite (8 mg) in methanol (2 mL) was stirred at room temperature. After completion of the reaction (monitored by TLC), the catalyst was filtered off and the solvent was evaporated under reduced pressure. The crude product was purified by column chromatography on silica gel to yield pure alcohols and phenols.

ACKNOWLEDGEMENTS

The authors are thankful to the University of Guilan Research Council for the partial support of this work.

REFERENCES

[1] LeBaron, P.C.; Wang, Z.; Pinnavaia, T.J, *Appl. Clay Sci.* **1999,** 15, 11-29.

[2] Pavlidou, S.; Papaspyrides, C, *Prog. Polym. Sci.* **2008,** 33, 1119-1198.

[3] Sinha Ray, S.; Okamoto, M, *Prog. Polym. Sci*. **2003,** 28, 1539-1641.

[4] Iliescu, R.I.; Andronescu, E.; Voicu, G.; Ficai, A.; Covaliu, C.I, *Appl. Clay Sci*. **2011,** 52, 62-68.

[5] Campbell, K.; Craig, D.Q.; McNally, T, *Int. J. Pharm*. **2008,** 363, 126-131.

[6] Anirudhan, T.; Ramachandran, *M, Appl. Clay Sci*. **2007**, 35, 276-281.

[7] Lagaly, G, *Appl. Clay Sci*. **1999**, 15, 1-9.

[8] Wang, S. H.; Wang, K. H.; Dai, Y. M.; Jehng, J. M, *Appl. Surf. Sci.* **2013,** 264, 470-475.

[9] Zampori, L.; Stampino, P.G.; Cristiani, C.; Dotelli, G.; Cazzola, P, *Appl. Clay Sci*. **2010**, 48, 97-102.

[10] Zampori, L.; Stampino, P.G.; Cristiani, C.; Cazzola, P.; Dotelli, G, *Appl. Clay Sci*. **2010**, 50, 266-270.

[11] Ratna, D.; Abraham, T.; Karger-Kocsis, J, *J. Appl. Polym. Sci*. **2008**, 108, 2156-2162.

[12] Geng, Y.; Wang, G.; Cong, Y.; Bai, L.; Li, L.; Yang, C, *J. Polym. Sci*., *Part B: Polym. Phys*. **2010,** 48, 106-112.

[13] Hoffmann, C.; Rabolt, J, *Macromolecules*. **1996,** 29, 2543-2547.

[14] Yu, J.; Wu, P, *Polymer*. **2007**, 48, 3477-3485.

[15] Kiasat, A.R.; Sayyahi, S, *Catal. Commun*. **2010,** 11, 484-486.

[16] Kiasat, A.R.; Badri, R.; Zargar, B.; Sayyahi, S, *J. Org. Chem*. **2008**, 73, 8382-8385.

 ACCEPTED MANUSCRIPT

[17] Jorapur, Y.R.; Rajagopal, G.; Saikia, P.J.; Pal, R.R, *Tetrahedron Lett*. **2008**, 49, 1495-1497.

[18] Choudhary, S.; Sengwa, R, *Indian J. Phys*. **2012,** 86, 335-340.

[19] Moreno, M.; Quijada, R.; Santa Ana, M.A.; Benavente, E.; Gomez-Romero, P.; González, G, *Electrochim. Acta*. **2011,** 58, 112-118.

[20] Sengwa, R.; Choudhary, S, *J. Macromol. Sci. B.* **2011,** 50, 1313-1324.

[21] Sengwa, R.; Choudhary, S, *Bull. Mater. Sci*. **2012,** 35, 19-25.

[22] Tang, C.; Hackenberg, K.; Fu, Q.; Ajayan, P.M.; Ardebili, H, *Nano Lett.* **2012,** 12, 1152-1156.

[23] Zhu, S.; Chen, J.; Li, H.; Cao, Y, Appl. Surf. Sci. **2013**, 264, 500-506.

[24] Kalbasi, R.J.; Massah, A.R.; Daneshvarnejad, B, *Appl. Clay Sci*. **2012**, 55, 1-9.

[25] Kocienski, P. J.; Enders, D.; Noyori, R.; Trost, B. M.; Eds., Protective Groups. Thieme, Stuttgart. **1994**, p. 191.

[26] Gryparis, C.; Stratakis, M, *Chem. Commun.* **2012**, 48, 10751--10753.

[27] Ghorbani-Choghamarani, A.; Norouzi, *M, Chin. J. Catal.* **2011**, 32, 595-598.

[28] Nikbakht, F.; Ghonche poor, E.; Ziyadi, H.; Heydari, A, *RSC* Adv. **2014**, 4, 34428-34434.

[29] Rostami, A.; Akradi, J.; Ahmad-Jangi, F, *J. Braz. Chem. Soc.* **2010**, 21, 1587-1592.

[30] Ziyaei-Halimjani, A.; Saidi, M, *J. Sci. I. R. Iran*. **2006**, 17, 123-126.

[31] Tillu, V.H.; Jadhav, V.H.; Borate, H.B.; Wakharkar, R.D, *Arkivoc*. **2004,** 14, 83-88.

[32] Kadam, S. T.; Kim, S. S, *J. Organomet. Chem.* **2009**, 694, 2562-2566.

[33] Zareyee, D.; Karimi, B, *Tetrahedron Lett*, **2007**, 48, 1277-1280.

[34] Zareyee, D.; Asghari, R.; Khalilzadeh, M.A, *Chin. J. Catal*. **2011**, 32**,** 1864-1868.

[35] Shirini, F.; Mamaghani, M.; Atghia, S. V, *Appl. Clay Sci*. **2012,** 58, 67-72.

[36] Shirini, F.; Mamaghani, M.; Atghia, S. V, *Catal. Commun.* **2011,** 12, 1088-1094.

[37] Shirini, F.; Abedini, M.; Pourhasan, R, *Dyes Pigments*. **2013**, 99, 250-255.

[38] Shirini, F.; Abedini, M.; Nasiri Abkenar, A.; Baghernejad, B, *J. Nanostruct. Chem.* **2014**, 4, 1-6.

[39] Shirini, F.; Abedini, M.; Pourhasan-Kisomi, R, *Chin. Chem. Lett*. **2014**, 25, 111-114.

[40] Shaterian, H. R.; Shahrekipoor, F.; Ghashang, M, *J. Mol. Catal. A: Chem.* **2007**, *272*, 142-151.

[41] Shirini, F.; Marjani, K.; Taherpour Nahzomi, H.; Zolfigol, M. A, *Phosphorus, Sulfur Silicon Relat. Elem.* **2008**, *183*, 168-177.

[42] Shirini, F.; Akbari-Dadamahaleh, S.; Mohammad-Khah, A.; Aliakbar, A. R, *C. R. Chimie***.** **2014**, 17, 164-170.

Table 1 Effect of HMDS and the PEG-SANM nanocomposite amounts on silylation of 4-chlorobenzyl alcohol (1 mmol) in acetonitrile (2 mL) at room temperature (reaction time: 4 min).

Entry	HMDS (mmol)	PEG-SANM nanocomposite(mg)	Convertion(%)	Isolated Yields (%)
1	0.75	0	No reaction	No reaction
2	0.75	10	100	98
3	0.5	10	100	98
4	0.5	8	100	98
5	0.5	5	100	90

 ACCEPTED MANUSCRIPT

Table2. Silylation of alcohols and phenols and deprotection of silyl ethers in the presence of the PEG-SANM nanocomposite at room temperature [a].

Entry	Substrate	Product	Ref.	Protection		Deprotection	
				Time (min)	Yield [b] (%)	Time (min)	Yield [b] (%)
1	$PhCH_2OH$	$PhCH_2OTMS$ (**2a**)	40	4	98	3	98
2	$4\text{-}ClC_6H_4CH_2OH$	$4\text{-}ClC_6H_4CH_2OTMS$ (**2b**)	41	4	98	2	98
3	$2\text{-}ClC_6H_4CH_2OH$	$2\text{-}ClC_6H_4CH_2OTMS$ (**2c**)	41	5	95	0.5	95
4	$2\text{-}BrC_6H_4CH_2OH$	$2\text{-}BrC_6H_4CH_2OTMS$ (**2d**)	41	4	95	4	92
5	$4\text{-}BrC_6H_4CH_2OH$	$4\text{-}BrC_6H_4CH_2OTMS$ (**2e**)	27	4	97	4	96
6	$2\text{-}NO_2C_6H_4CH_2OH$	$2\text{-}NO_2C_6H_4CH_2OTMS$ (**2f**)	41	8	93	5	91
7	$4\text{-}NO_2C_6H_4CH_2OH$	$4\text{-}NO_2C_6H_4CH_2OTMS$ (**2g**)	41	4	98	2	96
8	$2\text{-}MeC_6H_4CH_2OH$	$2\text{-}MeC_6H_4CH_2OTMS$ (**2h**)	41	4	98	0.5	97
9	$3,4\text{-}Cl_2C_6H_4CH_2OH$	$3,4\text{-}Cl_2C_6H_4CH_2OTMS$ (**2i**)	27	4	93	3.5	96
10	$4\text{-}Me_3CC_6H_4CH_2OH$	$4\text{-}Me_3CC_6H_4CH_2OTMS$ (**2j**)	35	4	90	4	90
11	$4\text{-}Me_2CHC_6H_4CH_2OH$	$4\text{-}Me_2CHC_6H_4CH_2OTMS$ (**2k**)	27	4	91	1	96
12	$3\text{-}MeOC_6H_4CH_2OH$	$3\text{-}MeOC_6H_4CH_2OTMS$ (**2l**)	35	4	92	0.5	96
13	$4\text{-}MeOC_6H_4CH_2OH$	$4\text{-}MeOC_6H_4CH_2OTMS$ (**2m**)	40	4	95	1	97
14	PhCH(OH)Ph	PhCH(OTMS)Ph (**2n**)	40	4	89	4	95
15	PhCH(OH)Me	PhCH(OTMS)Me (**2o**)	40	4	87	1.5	96

ACCEPTED MANUSCRIPT

16	$PhCH_2CH_2CH_2OH$	$PhCH_2CH_2CH_2OTMS$ (**2p**)	41	4	97	2	92
17	$PhCH_2CH_2OH$	$PhCH_2CH_2OTMS$ (**2q**)	40	4	98	2	91
18	$PhCH(Me)CH_2OH$	$PhCH(Me)CH_2OTMS$ (**2r**)	41	4	98	2	93
19		(**2s**)	40	10	90	9	93
20		(**2t**)	35	7	90	8	91
21		(**2u**)	40	25	95	20	94
22		(**2v**)	40	23	93	20	96
23	$PhCH = CHCH_2OH$	$PhCH = CHCH_2OTMS$ (**2w**)	41	6	96	5	96
24	$PhCH(OH)\ CH_2OH$	$PhCH(OTMS)\ CH_2OTMS$ (**2x**)	35	7	97 [c]	5	95 [d]
25	$4\text{-}EtC_6H_4OH$	$4\text{-}EtC_6H_4OTMS$ (**2y**)	35	5	90	10	93
26	$4\text{-}Me_2CHC_6H_4OH$	$4\text{-}Me_2CHC_6H_4OTMS$ (**2z**)	35	8	98	10	91
27	$4\text{-}ClC_6H_4NH_2$	$4\text{-}ClC_6H_4NHTMS$	-	30	0 [e]	-	-
28	$4\text{-}MeC_6H_4NH_2$	$4\text{-}MeC_6H_4NHTMS$	-	30	0 [e]	-	-
29	$4\text{-}MeC_6H_4SH$	$4\text{-}MeC_6H_4STMS$	-	30	0 [e]	-	-
30	$4\text{-}BrC_6H_4SH$	$4\text{-}BrC_6H_4STMS$	-	30	0 [e]	-	-
31	$4\text{-}ClC_6H_4CH_2OH$ +4-$MeC_6H_4NH_2$	$4\text{-}ClC_6H_4CH_2OTMS$ + 4-MeC_6H_4NHTMS	-	10	100 [f]0	-	-
32	$2\text{-}ClC_6H_4CH_2OH$ + $4\text{-}MeC_6H_4NH_2$	$2\text{-}ClC_6H_4CH_2OTMS$ + 4-MeC_6H_4NHTMS	-	10	100 [f]0	-	-
33	$4\text{-}MeOC_6H_4CH_2OH$ + $4\text{-}MeC_6H_4SH$	$4\text{-}MeOC_6H_4CH_2OTMS$ +$4\text{-}MeC_6H_4STMS$	-	10	100 [f]	-	-
34	$4\text{-}ClC_6H_4CH_2OH$ + $4\text{-}BrC_6H_4SH$	$4\text{-}ClC_6H_4CH_2OTMS$ + 4-BrC_6H_4STMS	-	10	100 [f]0	-	-

[a]The products were characterized by IR spectra, physical data, and comparison with the data reported in the literature.

[b]Isolated yield.

[c]1.0 mmol of HMDS and 16 mg of PEG-SANM were used.

[d]16 mg of PEG-SANM was used.

[e]The starting material was recovered intact.

[f]Conversion (%).

 ACCEPTED MANUSCRIPT

Table 3. Comparison of the catalytic efficiency of the PEG-SANM nanocomposite with other reported catalysts for the silylation of benzyl alcohol (1.0 mmol) using HMDS.

Entry	Catalyst (amount)	HMDS (mmol)	Reaction conditions	Time (min)	Yield (%)	Ref.
1	PEG-SANM nanocomposite (8 mg)	0.5	r.t./ CH_3CN	4	98	this work
2	Boric Acid (6.2 mg)	0.8	r.t./ CH_3CN	90	90	[29][a,c,d]
3	SiO_2-Cl (50 mg)	0.7	r.t./ Neat	20	98	[30][a,b,d]
4	SBA-15-Ph-Pr-SO_3H (19 mg)	0.6	35°C/ CH_2Cl_2	20	100	[34][a,b]
5	SANM (20 mg)	0.75	r.t./ CH_3CN	5	95	[35][b,d]
6	$HClO_4$--SiO_2 (50 mg)	0.8	r.t./ CH_3CN	2	98	[40][b,d]
7	RiH (80 mg)	0.75	r.t./ CH_3CN	5	94	[42][b,d]

Drawbacks:

[a]Long reaction times.

[b]High catalyst loading.

[c]Low yields.

dUse of excess amounts of HMDS.

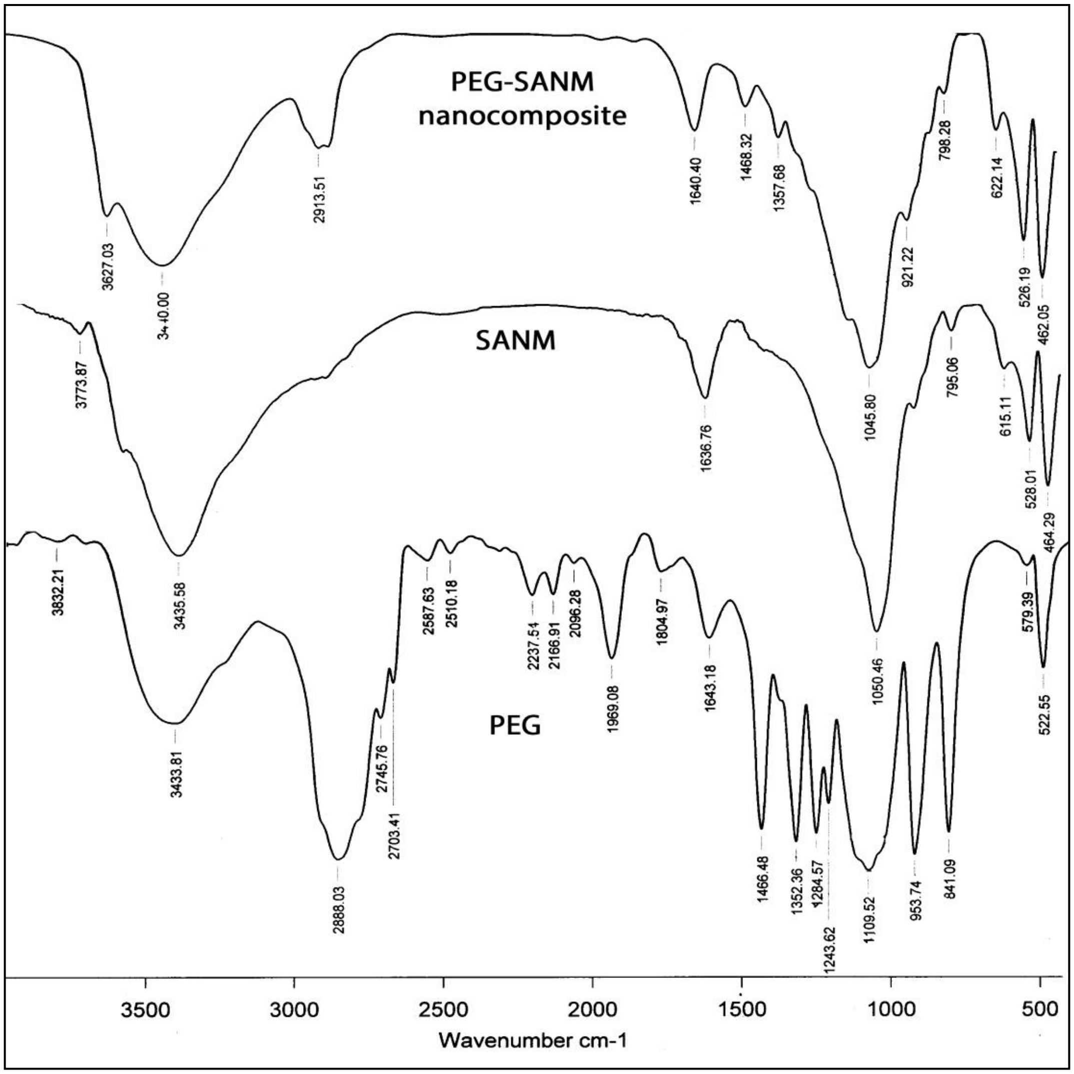

Fig. 1 FT-IR spectra of PEG, SANM and the PEG-SANM nanocomposite.

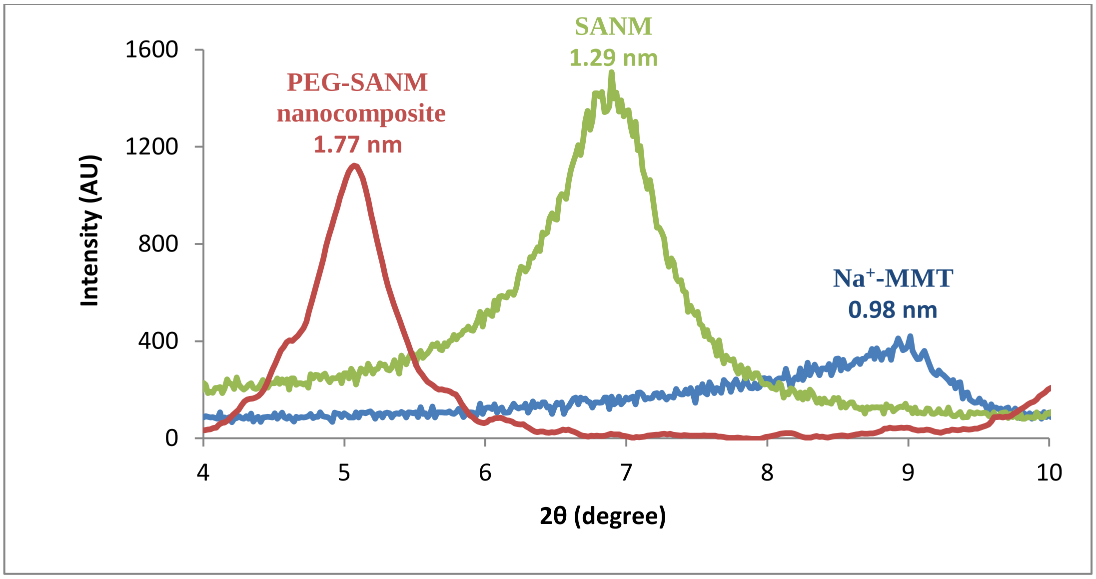

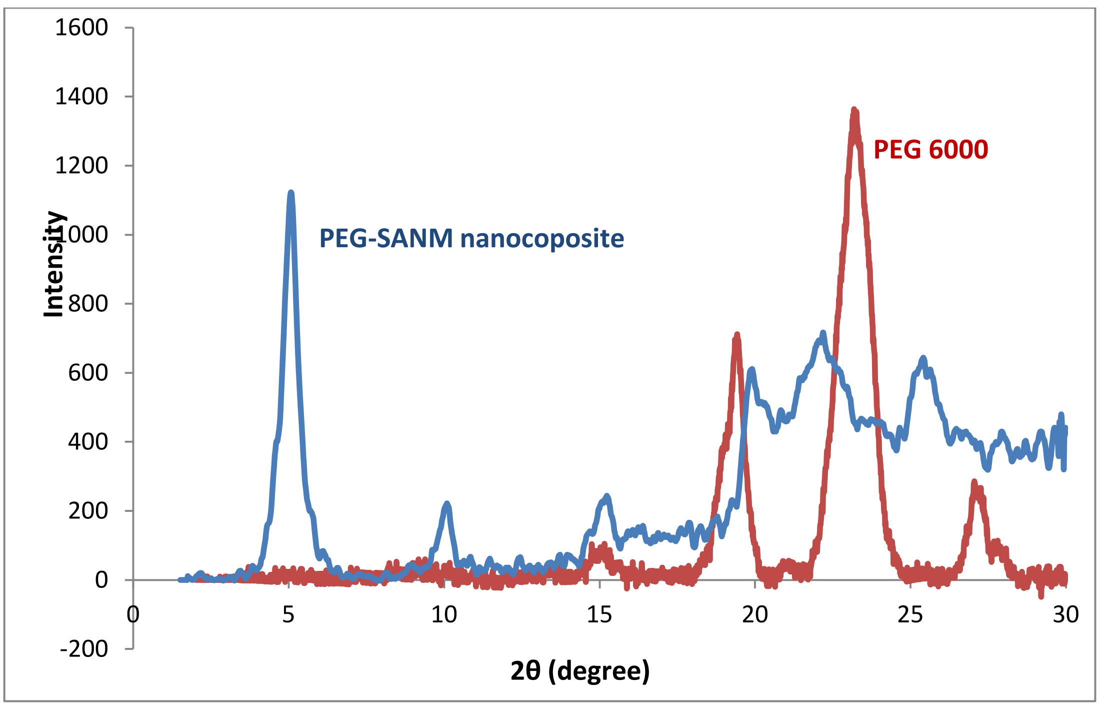

Fig. 2 The powder XRD patterns of the PEG-SANM nanocomposite, SANM, and Na^{+}-MMT (up) and the PEG-SANM nanocomposite and PEG-6000 (down).

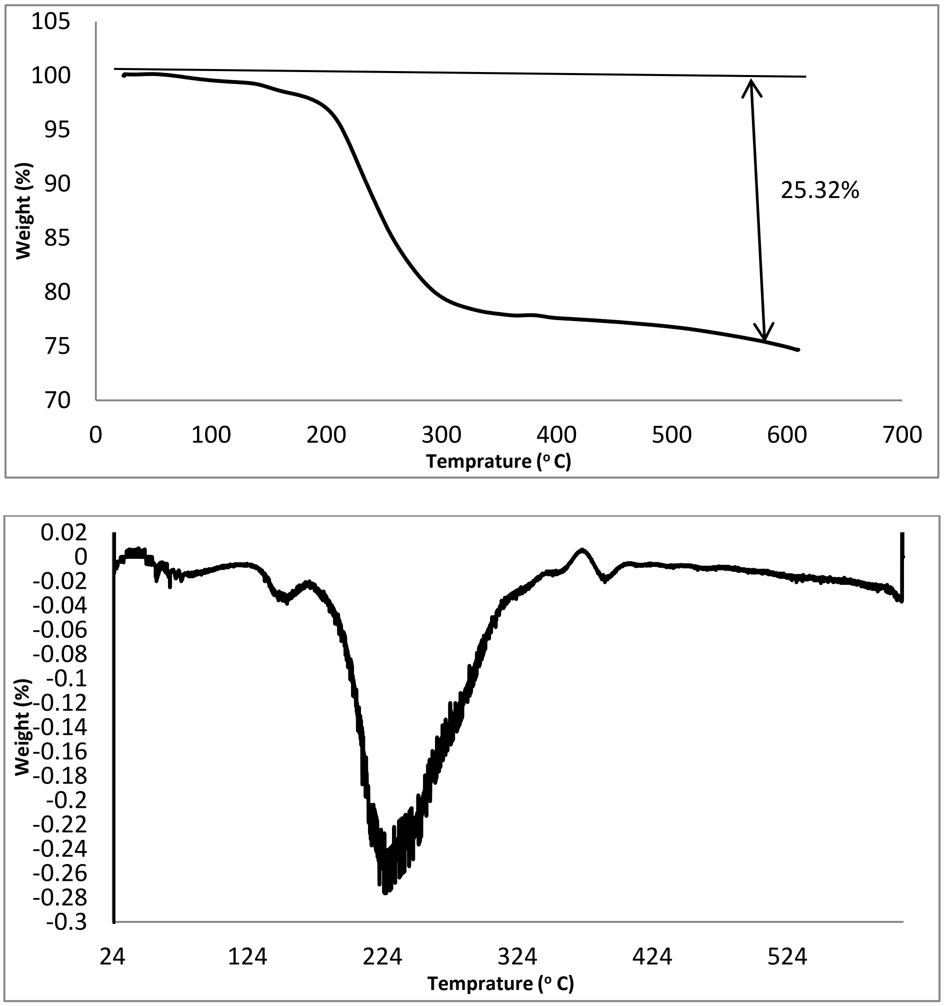

Fig. 3 TGA and DTG curves of the PEG-SANM nanocomposite.

$$\underset{\mathbf{1}}{\mathbf{ROH}} \xrightleftharpoons[\text{PEG-SANM (8 mg), MeOH, r.t.}]{\text{PEG-SANM (8 mg), HMDS (0.5 mmol), CH}_3\text{CN (2 mL), r.t.}} \underset{\mathbf{2a\text{-}z}}{\mathbf{ROTMS}}$$

SCHEME 1

ACCEPTED MANUSCRIPT